

PROBABILISTIC ESTIMATION OF LOW ENERGY ELECTRON TRAPPING IN QUADRUPOLES

K. G. Sonnad, J. A. Crittenden, CLASSE, Cornell University, Ithaca, NY, USA

Abstract

Electron cloud formation in quadrupoles is important for storage rings because they have the potential of being trapped for a time period that exceeds the revolution period of the beam. This can result in a turn by turn build up of cloud, that could potentially interfere with beam motion. Using the theory on the motion of particles in nonuniform magnetic fields, we describe a method to estimate the probability distribution of trapping across the cross-section of a quadrupole for a given field gradient and electron energy. Such an estimate can serve as a precursor to more detailed numerical studies of electron cloud build and trapping in quadrupoles.

INTRODUCTION

The trapping of electrons in quadrupoles has been observed in positron as well as proton rings [1, 2]. Calculation of trajectories of single electrons in quadrupoles has shown that they can indeed remain trapped indefinitely provided certain initial conditions are satisfied. [3, 4]. The motion of a charged particle travelling in a non-uniform magnetic field is said to be adiabatic if the condition $|\nabla B|/B|r_c \ll 1$, where B is the magnitude of the magnetic field and r_c is the cyclotron radius corresponding to this magnetic field. Under these conditions, the magnetic moment given by $\mu = mv_{\perp}^2/2B$ is an adiabatic invariant and is a conserved quantity, where v_{\perp} is the component of the velocity perpendicular to the magnetic field. The energy $\mathcal{E} = 1/2m(v_{\perp}^2 + v_{\parallel}^2)$ is always a conserved quantity. As the particle migrates to a region of higher magnetic field, the parallel component of the velocity v_{\parallel} reduces and a point may reach when it goes to zero, in which case the particle reverses its path. Based on this phenomenon, one can specify a so called loss cone drawn in velocity space. The axis of the cone is along v_{\parallel} . It can then be shown (see for example Ref [5]) that the angle of this cone θ_c satisfies $\sin^2 \theta_c = B_0/B_e$, where B_0 is the magnitude of the magnetic field at the initial point, and B_e corresponds to the field at the escape point, along the field line. If at the initial point, the particle lies outside the loss cone, it would reverse its path before reaching the escape point. Due to the symmetry in a quadrupole field pattern, it is guaranteed that two such "mirror" points occur along a field line, between which a particle may remain trapped. For trapping to occur, it is sufficient for two conditions to be satisfied. (1) The motion needs to remain adiabatic all along the field line, and (2) the particle needs to lie outside the loss cone at the given point on the field line. Reference [3] studied the nature of the particle trajectories and their escape when either conditions (1) or (2) were individually violated.

METHOD OF COMPUTING THE TRAPPING PROBABILITY

If the magnetic moment $\mu = mv_{\perp}^2/2B$ is conserved, then the perpendicular velocity of a particle travelling from point 1 to 2 can be traced, and is given by

$$v_{\perp}(2) = v_{\perp}(1) \left(\frac{B(2)}{B(1)} \right)^{1/2} \quad (1)$$

For a quadrupole field, the magnetic field is given by $B_x = ky$, $B_y = kx$, or $|\nabla B| = k$. Thus, condition for adiabatic motion to exist is

$$\frac{r_c |\nabla B|}{B} = \frac{v_{\perp} m k}{e B^2} \ll 1 \quad (2)$$

If the angle made by the particle with respect to the "perpendicular" direction is ϕ , then we have

$$v_{\perp} = v \cos(\phi) \quad (3)$$

For a particle to remain trapped, it is necessary that the motion remains adiabatic all along the field line. It is sufficient for this condition to satisfy if the motion is adiabatic at the point where the magnitude of magnetic field is a minimum. Using this, the condition for adiabatic motion to sustain along a field line may be obtained by combining equation (1) and (2). This is

$$\frac{v \cos(\phi) m k}{e B_o^{1/2} B_{min}^{3/2}} \ll 1 \quad (4)$$

Where B_o is field at the reference point, and B_{min} is the minimum field value along that field line. While there is no rule that demarcates between adiabatic and nonadiabatic motion, it would be reasonable for our purposes to make an assumption that the motion is adiabatic if the left side is less than a predefined empirical parameter $\eta \ll 1$. With this, Eq(4) will lead to the condition

$$\cos(\phi) < \frac{\eta e B_o^{1/2} B_{min}^{3/2}}{m v k} \quad (5)$$

We will now define another cone in velocity space whose axis is parallel to v_{\perp} , with angle ϕ_a , such that for all points lying inside this cone, the above condition is violated. Under our assumptions, these points correspond to cases where the particle motion will eventually cease to remain adiabatic. This gives us,

$$\cos(\phi_a) = \begin{cases} \frac{\eta e B_o^{1/2} B_{min}^{3/2}}{m v k}, & \text{if } \leq 1 \\ 0, & \text{otherwise} \end{cases} \quad (6)$$

Figure 1 shows the three regions in velocity space a particle may belong to. The regions are three dimensional with conical boundaries, while the figure is a projection on to a plane. For particles with an isotropic velocity distribution, and given energy, the probability of trapping is the fractional solid angle covered by the shaded region. There are three cases that need to be considered. (1) If $\cos(\phi_a) = 1$, the motion is adiabatic everywhere, and the trapping probability is $\cos(\theta_c)$. (2) If $\theta_c + \phi_a \geq \pi/2$, the region of trapping does not exist, and the trapping probability is zero. (3) If $\theta_c + \phi_a < \pi/2$ then the trapping probability is $\cos(\theta_c) - \sin(\theta_a)$. These values can easily be obtained by working out the fractional solid angles covered by the respective regions.

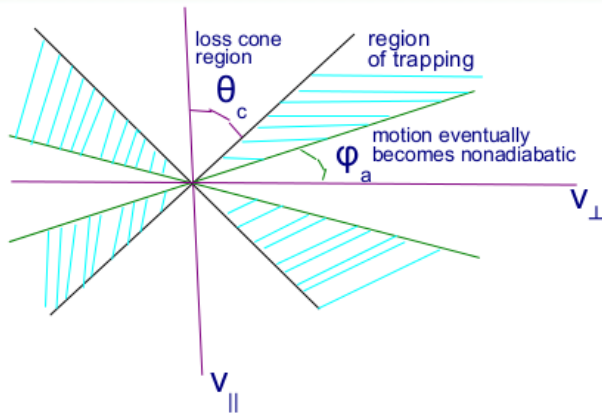


Figure 1: Regions in velocity space that will determine the nature of the particle trajectory.

The procedure to carry out the computation is as follows. The cross-section of the quadrupole region is divided into a grid. The magnetic field line passing through each point, lying at the center of the grid cell is traced. The tracing can be done using the method of direction cosines, where for a give step size Δs along the field line, the corresponding steps Δx and Δy are given by

$$\Delta x = \frac{B_x}{B} \Delta s \quad \Delta y = \frac{B_y}{B} \Delta s \quad (7)$$

In the process of scanning the whole field line between the two escape points, the values of the field at the escape point B_e as well as the minimum field value B_{min} are recorded. As long as the quadrupole chamber cross-section geometry is symmetric about the field pattern, the value of the two escape points are equal. If this is not the case, the smaller value between the two needs to be recorded. Using the formulation described in this paper, the values of $\sin(\theta_c)$ and $\cos(\phi_a)$ are computed. The trapping probability corresponding to the point of interest may then be computed based on the values of θ_c and ϕ_a and the procedure described in this section. The parameter η needs to be just sufficiently less than 1 so that higher order terms in η can be disregarded. Our computations showed that a change in this value within a range of 0.1-0.3 would only slightly alter the boundary that surrounds the so called "escape zone" described later in the paper.

5: Beam Dynamics and EM Fields

D03 - Calculations of EM fields - Theory and Code Developments

COMPUTATIONS FOR VARYING ENERGIES AND FIELD GRADIENTS

In this paper, this computational procedure is applied to the quadrupole magnets within the sections which have a circular cross-section in the Cornell Electron-Positron Storage Ring (CESR). The radius of the cross-section is 4.45 cm. The field gradient k of these quadrupoles is 7.3 T/m, while we use other values of k as well in order to study the dependence of trapping probability with field strength. In all our computations, we set the the grid cell size such that the radius along the vertical and horizontal axis get divided into 600 points, resulting in a total of 31205 cells. The step size along the field line Δs used here was 4.45×10^{-2} cm. The parameter η was set to 0.1, which seemed reasonable based on repeating certain calculations with varying values of η .

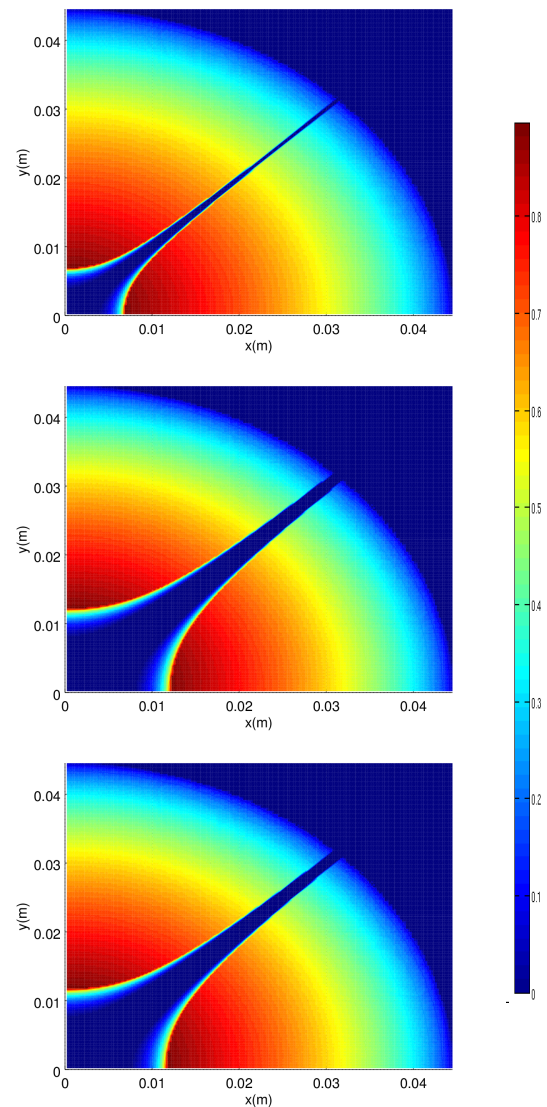


Figure 2: A map of the trapping probability for 100 eV electrons, $k = 7.3$ T/m (top), 1 KeV electrons $k = 7.3$ T/m (middle), 100 eV electrons, $k = 2.5$ T/m (bottom).

Figure 2 shows the results of the computation carried out for three cases. Due to the symmetry in the field and cross-section, it is sufficient to show one quadrant of the cross-section. The figure shows a clear region along the 45° line from the center, where the particles have no chance of being trapped. This region, which we refer to as an "escape zone", have field lines that pass very close to the center, where the magnitude of the field approaches zero. This corresponds to large values of ϕ_a . When the field magnitude diminishes, particles are expected to lose adiabaticity and the motion becomes irregular. With irregular motion, particles will enter the loss cone at some instance of their wandering and eventually escape. Such a case has been computed and clearly illustrated in [3]. The figures also show how the "escape zone" becomes wider with either increasing energy, or decreasing field.

Table 1 provides the values of the probabilities integrated over the cross-section of the chamber. The calculations were performed for varying electron energies and field gradients. These values represent the overall fraction of trapped particles for an initial particle distribution, that is uniform in position space and isotropic in velocity space.

Table 1: Probabilities Integrated over the Cross-section

	10 T/m	7.5 T/m	2.5 T/m
10 eV	0.5147	0.50828	0.48963
100 eV	0.4878	0.47012	0.42253
1 KeV	0.4178	0.37447	0.26881

The calculations made in this paper disregard certain effects. These include the finite length of the quadrupole segment and the consequences of longitudinal drift of the particles. Space charge effects and effects of the beam passage are not accounted for. In addition, the initial distribution need not be uniform in position and isotropic in velocity. Also, the choice of the parameter η introduces a degree of uncertainty. On the other hand, it has been shown [3,4] that escape of particles from longitudinal drift is not likely within one beam revolution period for typical energies (100eV). One can expect that space charge will not be significant once sufficient number of particles escape and the particle density tapers down. Changing η within a reasonable range only slightly altered the boundaries of the escape zone. A direct comparison between the results of this paper and a full build up and PIC simulation is not possible. However the calculations of this paper provide useful insight on the underlying physics not apparent in the full build up simulations.

UPCOMING EXPERIMENTS

The CESR Test Accelerator project [6] has installed a purpose-built quadrupole magnet and instrumented vacuum chamber [7] for measurements of electron cloud trapping to be performed during the December, 2016, running period. Following up on its initial observation of cloud trapping in a positron storage ring of 2013/4 [1], this addition of a

56-cm-long magnet adjacent to one of the original CESR quadrupoles of the same length will enable measurements of cloud trapping as a function of field gradient by compensating one field with the other. The 2013/4 measurements were made at a field gradient of 7.3 T/m, finding a long-term trapping fraction of about 7%. The new configuration will permit measurements up to a field strength of 3.5 T/m. Numerical PIC simulations tuned to the previous measurements predict a remarkably strong dependence of trapping fraction on field strength, finding maximum trapping of more than 30% at a field gradient near 1 T/m [8]. The vacuum chamber is instrumented with time-resolving electron detectors of the type used for the measurements of Ref. [1], but with triple the azimuthal coverage, as well as with a microwave pickup geometry which will allow cross-calibration of the electron collection and frequency-shift methods of cloud detection.

REFERENCES

- [1] M.G. Billing, J. Conway, E.E. Cowan, J.A. Crittenden, W. Hartung, J. Lanzoni, Y. Li, C.S. Shill, J.P. Sikora, and K.G. Sonnad, "Measurement of electron trapping in the Cornell Electron Storage Ring," *Phys. Rev. ST Accel. Beams*, vol. 18, p. 041001.
- [2] R.J. Macek, A.A. Browman, J.E. Ledford, M.J. Borden, J.F. O'Hara, R.C. McCrady, L.J. Rybarczyk, T. Spickermann, T.J. Zaugg, and M.T.F. Pivi, "Electron cloud generation and trapping in a quadrupole magnet at the Los Alamos proton storage ring," *Phys. Rev. ST Accel. Beams*, vol. 11, p. 010101, 2008.
- [3] E.E. Cowan, K.G. Sonnad, and S. Veitzer, "Trajectories of low energy electrons in particle accelerator magnetic structures," in *Proc. of the 25th Particle Accelerator Conference (PAC-2013)*, Pasadena, CA, 2013, p. 475.
- [4] L.F. Wang, H. Fukuma, S. Kurokawa, and K. Oide, "Photoelectron trapping in quadrupole and sextupole magnetic fields", *Phys. Rev. E*, vol. 66, p. 036502, 2002.
- [5] F.F. Chen, "Introduction to Plasma Physics and Controlled Fusion," 2nd ed., Vol. 1: Plasma Physics: Plenum Press, New York, 1984.
- [6] G.F. Dugan, M.A. Palmer & D.L. Rubin, "ILC Damping Rings R&D at CEsR-TA," *ICFA Beam Dynamics Newsletter*, J. Urakawa, Ed., International Committee on Future Accelerators, No. 50, p. 11–33, Dec. 2009.
- [7] J. P. Sikora *et al.*, "Design of an Electron Cloud Detector in a Quadrupole Magnet at CESR-TA," in *Proc. of the 5th International Beam Instrumentation Conference (IBIC 2016)*, Barcelona, Spain, 2016, paper WEPG35.
- [8] J. Crittenden *et al.*, "Progress in Detector Design and Installation for Measurements of Electron Cloud Trapping in Quadrupole Magnetic Fields at CEsR-TA," in *Proc. of the 7th International Particle Accelerator Conference (IPAC2016)*, Busan, Korea, 2016, paper WEPMW004.